Composite Structures 200 (2018) 165–172

Contents lists available at ScienceDirect

Composite Structures

journal homepage: www.elsevier.com/locate/compstruct

Broadband locally resonant metamaterial sandwich plate for improved noise insulation in the coincidence region

Zibo Liu[a,*], Romain Rumpler[a,b], Leping Feng[a]

[a] The Marcus Wallenberg Laboratory for Sound and Vibration Research (MWL), Department of Aeronautical and Vehicle Engineering, KTH Royal Institute of Technology, SE-100 44 Stockholm, Sweden

[b] Centre for ECO2 Vehicle Design, KTH Royal Institute of Technology, SE-100 44 Stockholm, Sweden

ARTICLE INFO

Keywords:
Acoustic metamaterial
Sandwich plate
Sound transmission loss
Coincidence frequency

ABSTRACT

A new design for locally resonant metamaterial sandwich plates is proposed in this paper for noise insulation engineering applications. A systematic method to tune the resonance frequency of local resonators is developed in order to overcome the coincidence phenomenon. This method, based on an impedance approach, additionally explains the ability to overcome the antiresonance associated with these local resonators. The influence of the radiated sound from these local resonators is further investigated with finite element (FE) models, particularly in connection with the sound transmission loss (STL) of the resulting metamaterial sandwich plates. The new sandwich design proposed emerges from these analyses, encapsulating the resonators inside the core material. In addition to overcoming the coincidence effect and limiting the noise radiation by the resonators, the proposed design allows to improve the mass ratio of the metamaterial sandwich structure. This, in turn, enables to broaden the working frequency band independently of the material adopted for the resonator. The proposed metamaterial sandwich plate thus combines improved acoustic insulation properties, while maintaining the lightweight nature of the sandwich plate and its good static properties.

1. Introduction

Sandwich structures are widely used in modern engineering due to their low mass and high stiffness. However, these good static properties may come at the expense of the acoustic properties, such as noise shielding capability, which has become an essential issue in engineering designs as the demand grows for a better acoustic environment.

The bad STL of a sandwich plate often occurs in the coincidence frequency range, which is much wider than for a single-layer homogeneous plate. In addition, the coincidence frequency range for sandwich plates often drops into the audible frequency range. One reason for these undesirable acoustic properties is that the bending stiffness of the sandwich plate decreases with increasing frequencies. As a result, a range of coincidence frequencies may appear instead of a typical coincidence frequency for a single layer plate, that is, the bending wave speed in the sandwich panel and the trace wave speed in the surrounding medium may remain close over a broader frequency range.

It is therefore of great interest to improve the acoustic properties of such sandwich panels. Extensive research has been conducted over the past few decades regarding the acoustic behavior and improvement of the acoustic properties of sandwich plates [1–8]. In addition to the conventional design methods, the concept of acoustic metamaterials has recently been adopted in order to further improve the noise shielding acoustic properties of plates including sandwich plates, sometimes referred to as 'metamaterial plates'.

As first proposed by Z. Liu [9], acoustic metamaterials have been given great attention due to their exotic acoustic properties [10,11]. They normally refer to artificial composites which possess acoustic properties that do not exist in nature. Locally resonant materials are one type among the various types of acoustic metamaterials. They are in principle made of periodically organized lattices, whose periodicity is much smaller than the acoustic wavelength. The local phenomenon, *e.g.* local resonance, within each lattice, may lead to nontrivial effective acoustic properties of the entire structure, *e.g.* displaying effective negative mass [12] over some targeted working frequency bands, and can thus be used in order to prevent or abnormally manipulate the propagation of acoustic waves [13–25].

Such locally resonant systems, or metamaterial plates, consist of stepped resonators periodically distributed on a host plate. These resonators, mounted onto the host plate, introduce local resonances at specifically targeted frequencies. Several studies have been conducted concerning locally resonant metamaterial plates consisting of a single-

* Corresponding author.
E-mail addresses: zibo@kth.se (Z. Liu), rumpler@kth.se (R. Rumpler), fengl@kth.se (L. Feng).

https://doi.org/10.1016/j.compstruct.2018.05.033
Received 23 January 2018; Received in revised form 28 April 2018; Accepted 7 May 2018
Available online 16 May 2018

layer homogeneous plate as a host plate [26–29,21,24]. In these studies, the Bloch wave vectors are used to describe the wave propagation in the plate. Metamaterial sandwich structures including beams [30] and plates [31] have also been studied. These studies have confirmed that the metamaterial plate design is an effective technique to improve the STL property. Furthermore, the mass ratio of the resonators to the host plate is shown to be a critical property in order to broaden the working frequency band.

However, in these previous contributions, the stepped resonators are considered to be attached to the surface of the host plate. There may be several drawbacks to this configuration. First, the natural way to increase the mass ratio without changing the properties of the host plate is then to increase the mass of the resonators, which however increases the overall weight of the structure. In addition, placing the resonator on the surface of the plate may not be practical for realistic applications where the surface of the plate may fulfill other functional requirements. Finally, the radiation from the resonators may adversely affect the STL behavior, especially when the resonators become relatively large in size. To the knowledge of the authors, this impact of the radiation effect from the stepped resonators has not been introduced in previous studies.

In order to overcome these potential drawbacks, a configuration with an embedded resonator is proposed for sandwich plates. By introducing an air cavity inside the core material of the sandwich plate, the resonator may be placed inside the sandwich plate. Several advantages can be expected from such a configuration. First, the mass ratio may be easily increased, thus potentially leading to a significant broadening of the working frequency band. In addition, the STL properties may not be adversely affected by the sound potentially radiated from the resonators at resonance. More importantly, the design may be better suited for engineering applications requiring flat outer surfaces. This may allow to take full advantage of the sandwich plate properties, including its high stiffness and light weight, as well as its refined acoustic properties, especially in the frequency range where the coincidence phenomenon occurs.

The present contribution evaluates the potential of the design of such locally resonant metamaterial sandwich plates in order to improve the STL properties in the coincidence region. It consists both in theoretical developments, and further evaluations using FE simulations. First, in Section 2, a brief theoretical evaluation is made of the STL property of a thin plate, based on the impedance approach. The theoretical developments support the explanations for the STL behavior of the metamaterial single-layer/sandwich plates. A criterion is established in order to systematically tune the resonance frequency of the resonator. Then, in Section 3, these developments are compared against existing models from the literature, and results from FE simulations, assuming resonators mounted on the surface. These FE results allow to make an investigation of the adverse radiation effect from the stepped resonators. On the basis of these evaluations, a new configuration of the metamaterial sandwich plate is proposed in Section 4. The results associated with this new configuration are compared with those of conventional designs, highlighting its potential for noise insulation purposes.

2. Impedance approach

In this section, the STL and the principle of designing the working frequency band of the metamaterial plate are presented. These theoretical developments are done from the point of view of the plate impedance, assuming a thin plate. The analysis is carried out on an unbounded plate surrounded by two semi-infinite acoustic domains consisting of air. The plate is excited by an incident plane wave with an elevation angle θ with respect to the normal direction of the plate. In addition, both the single-layer and sandwich plates are assumed to consist of isotropic materials, while the stepped resonator is simplified to an idealized mass-spring system. The impedance of the single-layer plate is first reviewed. On this basis, and in combination with the introduction of the effective mass theory for acoustic metamaterials, the effective impedance of the single-layer metamaterial plate is derived. The same steps are followed for the sandwich metamaterial plate. The bending motion alone is considered in the sandwich plate when establishing its impedance. The effective impedance derived for the sandwich metamaterial then allows to define a criterion in order to tune the resonance frequency of the stepped resonators.

The transmission coefficient of the plate under the thin plate assumption can be expressed as

$$\tau = \left| 1 + \frac{Z\cos\theta}{2\rho_0 c_0} \right|^{-2}, \tag{1}$$

where Z represents the corresponding plate impedance; ρ_0 and c_0 represent the density and the speed of sound in the air medium. The STL is calculated by

$$\mathrm{STL} = 10\log\left(\frac{1}{\tau}\right).$$

2.1. Single-layer plate

In the low frequency range, the bending wave in the plate is critical for the sound transmission performance. For a single-layer thin plate under acoustic excitation, the impedance of the plate is estimated as [32]

$$Z_0 = \frac{\Delta p}{\hat{v}} = j\omega m\left(1 - k^4\frac{D}{\omega^2 m}\sin^4\theta\right) = j\omega m\left(1 - \frac{k^4}{\kappa^4}\sin^4\theta\right). \tag{2}$$

This follows from the continuity of normal velocities at the interface between the plate and the air medium together with Newton's second law, with Z_0 the impedance of the plate; Δp the pressure difference between the two sides of the plate; m and D the surface density and the bending stiffness of the plate respectively; $\kappa = (\omega^2 m/D)^{\frac{1}{4}}$ the bending wavenumber of the plate.

At the coincidence frequency, the wavenumbers associated with the bending wave in the plate and the trace wave are equal,

$$\kappa = k\sin\theta.$$

The coincidence frequency f_{co} and critical frequency f_c are then given by

$$f_{co} = \frac{1}{2\pi}\frac{{c_0}^2}{\sin^2\theta}\sqrt{\frac{m}{D}}; \quad f_c = \frac{{c_0}^2}{2\pi}\sqrt{\frac{m}{D}}. \tag{3}$$

Eq. (2) may subsequently be rewritten in terms of f_{co},

$$Z_0 = j\omega m\left(1 - \frac{f^2}{f_{co}^2}\right), \tag{4}$$

which implies that $Z_0 = 0$ when $f = f_{co}$. In other words, at the coincidence frequency, the impedance drops to zero, implying total transmission as can be seen from Eq. (1).

In a single-layer metamaterial plate, in the low frequency range, when the periodicity of the stepped resonator is much smaller than the wavelength considered, the mass of the entire structure may be treated as a frequency-dependent function. The total mass of the structure may thus be expressed by the effective mass theory [10,11], as

$$M_{\mathrm{eff}} = M + \frac{M_{\mathrm{R}}}{1 - f^2/f_{\mathrm{res}}^2},$$

where M, M_{R} are the mass of the host plate and the resonator, respectively; f_{res} is the resonance frequency of the locally resonant system. The effective surface density of the structure is then

$$m_{\mathrm{eff}} = \frac{M_{\mathrm{eff}}}{S} = m + \frac{m_{\mathrm{R}}}{1 - f^2/f_{\mathrm{res}}^2} = m\left(1 + \frac{\delta}{1 - f^2/f_{\mathrm{res}}^2}\right), \tag{5}$$

where S is the surface area of the lattice and $\delta = m_R/m$ is the mass ratio of the resonator to the host plate.

The effective impedance of the metamaterial plate Z_a is therefore estimated by introducing m_{eff} for the surface density m in Eq. (4),

$$Z_a = j\omega m\left(1 + \frac{\delta}{1-f^2/f_{res}^2}\right)\left(1-\frac{f^2}{f_{co}^2\left(1+\frac{\delta}{1-f^2/f_{res}^2}\right)}\right), \tag{6}$$

or

$$Z_a = j\omega m\left(1 + \frac{\delta}{1-f^2/f_{res}^2}-\frac{f^2}{f_{co}^2}\right). \tag{7}$$

2.2. Sandwich plate

The vibration motion of the sandwich plate can be decomposed into the in-phase modes and the out-of-phase modes [33]. In the low frequency range, of interest in the present work, the dynamic behavior is dominated by the in-phase modes. These are mostly controlled by the outer faces and the shear of the core of the sandwich [34]. For a propagation in the x direction, the wave equation may thus be given by

$$-2D_S D_f\frac{\partial^6 w}{\partial x^6} + 2D_f I_S\frac{\partial^6 w}{\partial t^2\partial x^4}-(D_S m + 2D_f m + I_S G_c t_c)\frac{\partial^4 w}{\partial t^2\partial x^2} + G_c t_c\left(D_S\frac{\partial^4 w}{\partial x^4} + m\frac{\partial^2 w}{\partial t^2}\right) + I_S m\frac{\partial^4 w}{\partial t^4} = 0, \tag{8}$$

where

$$D_f = \frac{E_f t_f^3}{12(1-\nu_f^2)},$$
$$D_S = \frac{E_c t_c^3}{12(1-\nu_c^2)} + \frac{E_f}{(1-\nu_f^2)}\left(\frac{t_c^2 t_f}{2} + t_c t_f^2 + \frac{2}{3}t_f^3\right),$$
$$G_c = \frac{E_c}{2(1+\nu_c)},$$
$$I_S = \frac{1}{12}\rho_c t_c^3 + \rho_f\left(\frac{t_c^2 t_f}{2} + t_c t_f^2 + \frac{2}{3}t_f^3\right).$$

The solution to Eq. (8) is assumed to be of the form $w = w_0 e^{j(\omega t - k_x x)}$, thus leading to the dispersion relation of the sandwich plate,

$$2D_S D_f k_x^6-2D_f I_S\omega^2 k_x^4-(D_S m + 2D_f m + I_S G_c t_c)\omega^2 k_x^2 + G_c t_c(D_S k_x^4-m\omega^2) + I_S m\omega^2 = 0 \tag{9}$$

The in-phase wavenumbers, $k_{1,2,3} = \pm\kappa_{1,2,3}$, may then be obtained, where $\kappa_{1,3}$ correspond to the evanescent waves in the low frequency range while κ_2 corresponds to the first in-phase propagating mode. Focusing on the propagating wave only, κ_2 corresponds to the bending wavenumber. The equivalent bending stiffness of the sandwich plate, which can also be simultaneously obtained [5], is a function of frequency and decreases with increasing frequencies.

In the low frequency range, where the bending wave is dominant, the impedance of the sandwich plate may also be expressed in a form similar to Eqs. (2)–(4), under the thin plate assumption,

$$Z_{S0} = j\omega m\left(1-\frac{k^4}{\kappa_2^4}\sin^4\theta\right) = j\omega m\left(1-\frac{f^2}{f_{Sco}^2}\right), \tag{10}$$

where

$$f_{Sco} = \frac{1}{2\pi}\frac{{c_0}^2}{\sin^2\theta}\frac{{\kappa_2}^2}{k}$$

is a function of frequency. A similar form also follows for the metamaterial sandwich plate,

$$Z_{Sa} = j\omega m\left(1 + \frac{\delta}{1-f^2/f_{res}^2}-\frac{f^2}{f_{Sco}^2}\right) \tag{11}$$

Note that, m_{eff} should be used in Eq. (9) in order to calculate the 'effective' bending wavenumber, and subsequently, the coincidence frequency of the metamaterial sandwich plate which is then used in Eq. (11).

2.3. Systematic tuning of the resonators

2.3.1. Suppression of the coincidence phenomenon

Total transmission occurs when the plate impedance is zero, or, by extension, when the effective impedance of the metamaterial is zero. For the single-layer plate, this translates into $Z_a = 0$, or

$$1 + \frac{\delta}{1-f^2/f_{res}^2}-\frac{f^2}{f_{co}^2} = 0. \tag{12}$$

For the solution to Eq. (12) to be real, f_{res} must satisfy

$$({f_{res}}^2-f_{co}^2)^2-4f_{res}^2 f_{co}^2\delta \geqslant 0, \tag{13}$$

which implies a resonance frequency such that

$$f_{co}(\sqrt{1+\delta}-\sqrt{\delta}) < f_{res} < f_{co}(\sqrt{1+\delta} + \sqrt{\delta}). \tag{14}$$

Under these conditions, the effective impedance will not reach zero, which prevents the coincidence phenomenon.

2.3.2. Improving the sound transmission loss around the coincidence frequency

It is sometimes not enough just to ensure that the effective impedance of the metamaterial plate exceeds zero, since the STL might still be less than that of the original base plate [28,29]. The following thus focuses on reconsidering the performance from a transmission perspective.

Neglecting the structural damping, the transmission coefficients of the original plate and the metamaterial plate, according to Eqs. (1), (4), and (7), are given by

$$\frac{1}{\tau_0} = 1 + \left(\frac{\cos\theta}{2\rho_0 c_0}\right)^2 |Z_0|^2, \tag{15a}$$

$$\frac{1}{\tau_a} = 1 + \left(\frac{\cos\theta}{2\rho_0 c_0}\right)^2 |Z_a|^2, \tag{15b}$$

since Z_0 and Z_a are purely imaginary in this case. The difference between these two terms is

$$\frac{1}{\tau_a}-\frac{1}{\tau_0} = \left(\frac{\cos\theta}{2\rho_0 c_0}\right)^2\left(2\left(1-\frac{f^2}{f_{co}^2}\right) + \frac{\delta}{1-f^2/f_{res}^2}\right)\frac{\delta}{1-f^2/f_{res}^2}. \tag{16}$$

If there is no intersection between the two transmission coefficients, *i.e.* $\frac{1}{\tau_a}-\frac{1}{\tau_0} \neq 0$, the STL of the metamaterial plate will be higher than that of the base plate. Since for frequencies approaching zero we have $STL_a \geqslant STL_0$, an analogous condition to Eq. (14) may be expressed,

$$f_{co}(\sqrt{1+\delta/2}-\sqrt{\delta/2}) < f_{res} < f_{co}(\sqrt{1+\delta/2} + \sqrt{\delta/2}). \tag{17}$$

Under the conditions of Eq. (17), the STL of the metamaterial plate is ensured to be better than that of the original plate for any frequency close or lower than the coincidence frequency. In our study, the resonant frequency is tuned to the corresponding coincidence frequency.

2.3.3. Bandwidth of the working frequency range

The bandwidth of the working frequency range can be evaluated by determining the frequencies associated with the local minima of the STL before (f_1) and after (f_2) the resonance frequency. These lead to

$$f_1 = f_{res}\sqrt{1-\frac{f_{co}}{f_{res}}\sqrt{\delta}}, \quad f_2 = f_{res}\sqrt{1+\frac{f_{co}}{f_{res}}\sqrt{\delta}}. \tag{18}$$

If the resonance frequency is tuned such that $f_{res} = f_{co}$, the normalized

Table 1
The parameters of the sandwich plate.

	Thickness (m)	E (Pa)	ν (–)	ρ (kg/m^3)	Loss factor η (–)
Face	t_f = 2e−3	6.9e10	0.3	2700	η_f = 1e−3
Core	t_c = 5e−2	8e8	0.3	920	η_c = 1e−2

working frequency range may then be expressed as

$$\frac{\Delta f}{f_{co}} = \frac{|f_2 - f_1|}{f_{co}} = \sqrt{1+\sqrt{\delta}} - \sqrt{1-\sqrt{\delta}} \sim \sqrt{\delta}. \tag{19}$$

The bandwidth is therefore approximately proportional to $\sqrt{\delta}$, which means that the working frequency range can be extended by increasing the mass ratio. The same conclusion may also apply to a sandwich plate, which has an analogous expression for the effective impedance, provided that the equivalent bending stiffness is a smooth function of frequency.

3. Surface-mounted resonator

Applications are presented for an aluminum or a sandwich plate as the host plate. The single-layer, aluminum plate has a thickness of 2 cm. The parameters for the sandwich host plate are shown in Table 1. The surface density of the host sandwich plate is 56.8 kg/m^2. Steel, lead and tungsten are chosen as potential materials for the stepped resonators. In addition, damping is included by introducing structural losses by means of the loss factor (and complex notation) for both the theoretical estimations and numerical simulations.

The numerical simulations are conducted based on the FE method and realized in the commercial software COMSOL®. The model is constructed for a single lattice of the structure, as shown in Fig. 1. The unbounded nature of the sandwich is modeled by applying Floquet periodic boundary conditions. Non-reflecting boundary conditions are implemented by setting plane wave radiation boundary conditions as illustrated in Fig. 1. The dimension of the mesh is set to be of the order of one sixth of the shortest wavelength in order to ensure the accuracy of the calculations. A convergence check allowed to ensure a proper refinement of the mesh. The STL is subsequently calculated according to Eq. (20) by considering the pressure difference between the two sides of the plate.

$$\mathrm{STL} = 20\log\left|\frac{p_{inc}}{p_{trans}}\right| \tag{20}$$

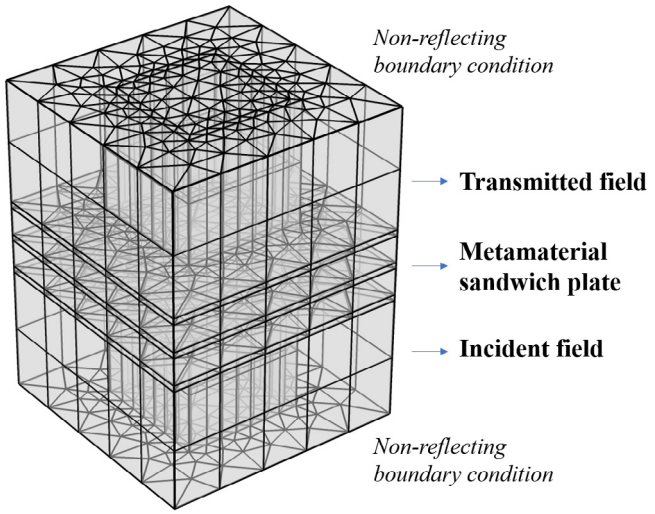

Fig. 1. The finite element model of the metamaterial sandwich plate constructed in COMSOL®.

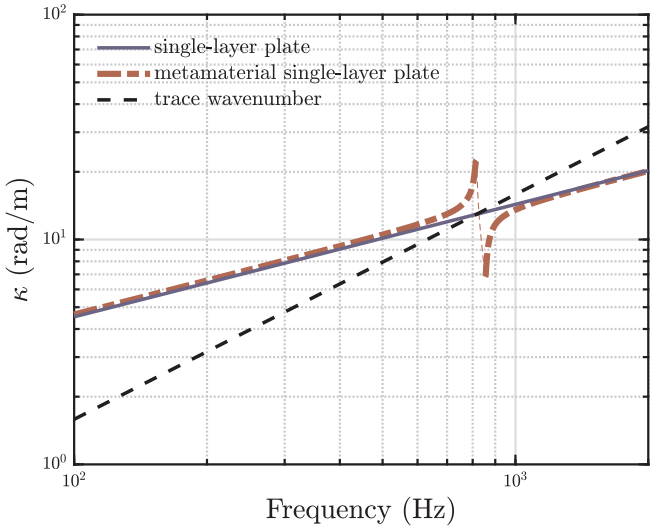

Fig. 2. Wavenumber of the single-layer plate and the metamaterial single-layer plate. The intersection represents where the coincidence phenomenon occurs.

For the theoretical model, the radiated sound from the resonators is omitted in the model since the metamaterial plate may be considered as 'homogeneous' in the low frequency range. However, it may still provide a fast and reliable way to tune the resonance frequency of the resonator in order to overcome the coincidence phenomenon. In that sense, it may be useful in a step leading to a costly and more detailed FE analysis, necessary for a further optimized design of the metamaterial sandwich plate.

3.1. Single-layer plate

The bending wavenumbers and the STL of the single-layer plate with and without stepped resonators are plotted against frequency in Figs. 2 and 3. These demonstrate the ability of the metamaterial design to compensate for the coincidence phenomenon. As can be seen, with the red curve, a gap appears in the plot of the bending wavenumber against frequency for the metamaterial plate. Because the intersection

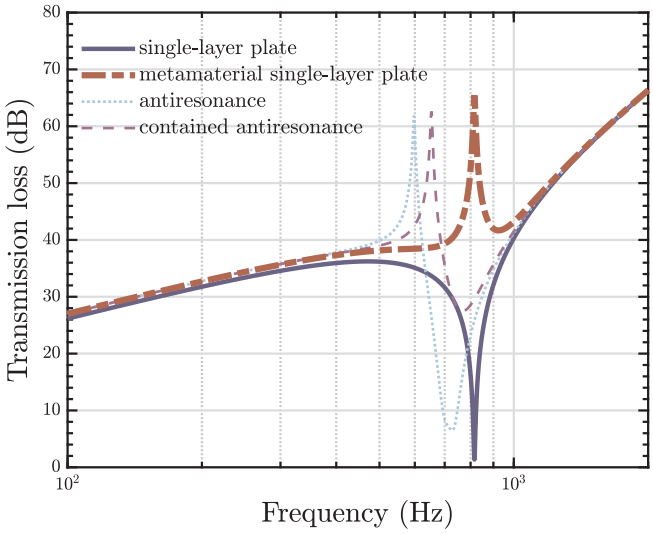

Fig. 3. Sound transmission loss of the single-layer plate and the metamaterial single-layer plate, with $\delta = 0.1$. Under-tuned resonance frequency: outside the suitable frequency range – Cyan-dotted line; inside the suitable frequency range – Magenta-dotted line; on the coincidence frequency – Red-solid line. (For interpretation of the references to colour in this figure legend, the reader is referred to the web version of this article.)

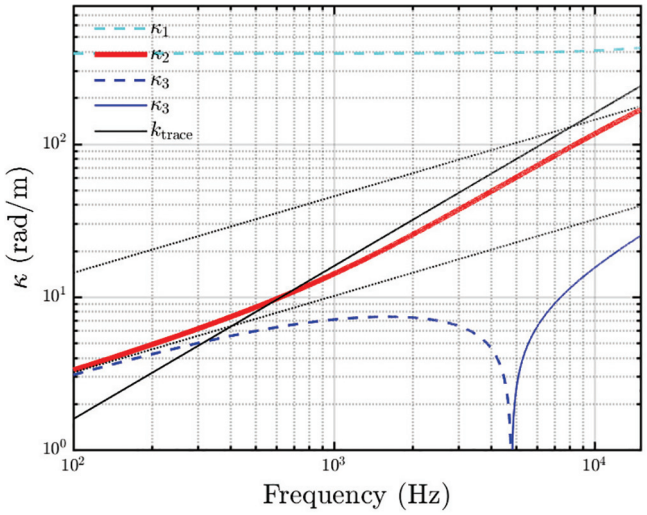

Fig. 4. In-phase wavenumbers of the sandwich plate estimated by Eq. (9). Evanescent waves (Dashed lines) and propagating waves (Solid lines). The upper and lower asymptotic dotted lines represent the bending wavenumbers of: *(i)* the face panel and *(ii)* the sandwich plate calculated using its static bending stiffness.

of the curves associated with the bending wavenumber and the trace wavenumber is avoided, the coincidence phenomenon is suppressed. Consequently, on the STL curve in Fig. 3, instead of the typical dip associated with the coincidence frequency, a sharp increase is observed. It is due to the sharp increase of the effective mass, as shown by Eq. (5).

The design methodology tested on a single-layer plate is further extended to the acoustic design of metamaterial sandwich plates in the following.

3.2. Sandwich plate

3.2.1. Sound transmission loss of the host sandwich plate

As aforementioned in Section 2.2, the acoustic waves propagating in the sandwich plate include in-phase propagating modes and anti-phase propagating modes. As shown in Fig. 4, in the low frequency range, the in-phase propagating modes are dominating the vibration of the sandwich plate. In this frequency region, only the wavenumber κ_2 is real. It corresponds to the bending wavenumber, which is of interest here. The intersection between the bending wavenumber and the trace wavenumber again corresponds to the coincidence phenomenon. The distinction, however, between the single-layer plate and the sandwich plate lies in the fact that the bending wavenumber of the sandwich plate may remain close to the trace wavenumber over a rather broad frequency range. This is due to the decrease of the bending stiffness of the sandwich with respect to frequency. The fact that the bending wavenumber is close to the trace wavenumber over a rather broad frequency range translates into bad acoustic properties of the sandwich plate, to be compensated by the introduction of stepped resonators.

The STL calculation, based on the impedance of the sandwich plate, is therefore reformulated introducing the bending wavenumber κ_2 only. The result is compared with Moore's theory [33] (see Fig. 5) in which both the in-phase and anti-phase modes are considered. The FE result is also plotted for validation. As shown in Fig. 5, the estimation leads to a satisfactory accuracy for the STL and for the coincidence frequency under the thin plate assumption in the low frequency range. With increasing frequencies, the anti-phase mode contribution is not negligible anymore, and the simplified model introduced deviates from Moores' theory and the FE results. In the range of interest, *i.e.* below and close to the coincidence region, the simplified model provides an acceptable description of the acoustic behavior, and is further developed for the metamaterial sandwich plate in the following.

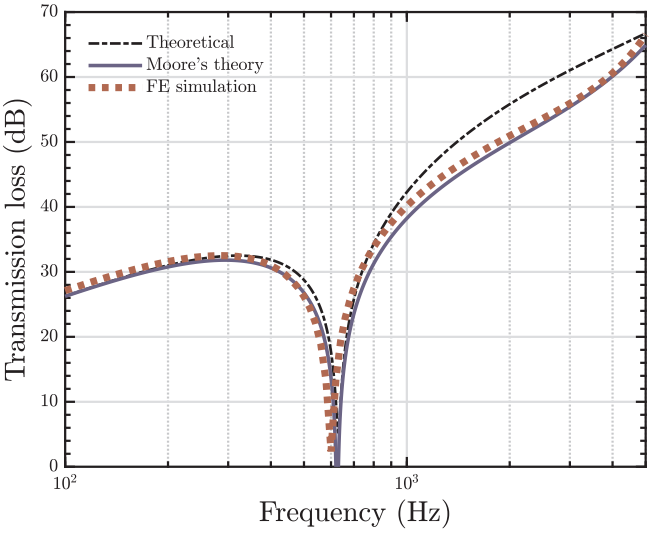

Fig. 5. Sound transmission loss of the sandwich plate estimated by the impedance approach, Moore's theory and finite element method.

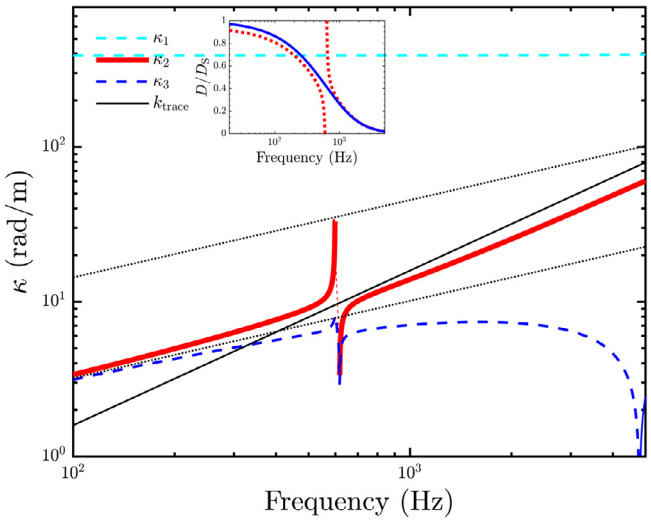

Fig. 6. Effective wavenumbers of the metamaterial sandwich plate, and effective bending stiffness (inserted plot).

3.2.2. Metamaterial sandwich plate

By analogy with the metamaterial single-layer plate, the effective bending wavenumber of the metamaterial sandwich plate is plotted in Fig. 6. The discontinuity observed is due to the discontinuity in the effective bending stiffness (see the plot inserted in Fig. 6). This is triggered by the locally resonant stepped resonators and the width of the gap is determined by the mass ratio of the stepped resonator to the host plate.

As shown in Fig. 7, the coincidence effect of the sandwich plate, reflected in the STL, may be overcome with the metamaterial design. The theoretical results correspond to the STL calculations where the effective bending wavenumber of the sandwich plate is introduced into the plate impedance. As observed for the single-layer case, the gap in the bending wavenumber over the coincidence frequency range theoretically allows a substantial improvement of the STL. The FE results, also plotted in Fig. 7, validate the theoretical developments up to the coincidence region. Beyond the coincidence frequency range, the deviations are, as explained in connection with Fig. 5, due to the increasing contributions from other modes of the sandwich plate besides the bending mode. Additionally, it is noteworthy at this stage that the peak values at the resonance frequency for the FE simulation and the

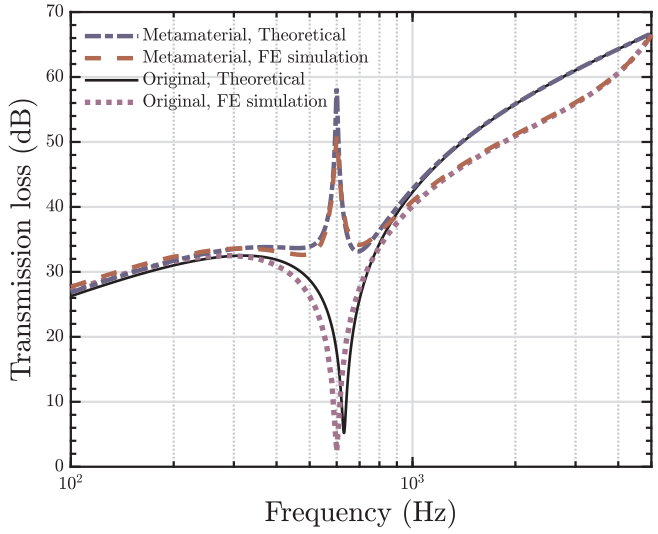

Fig. 7. Sound transmission loss of the original host sandwich plate and metamaterial sandwich plate based on the impedance approach and the finite element method.

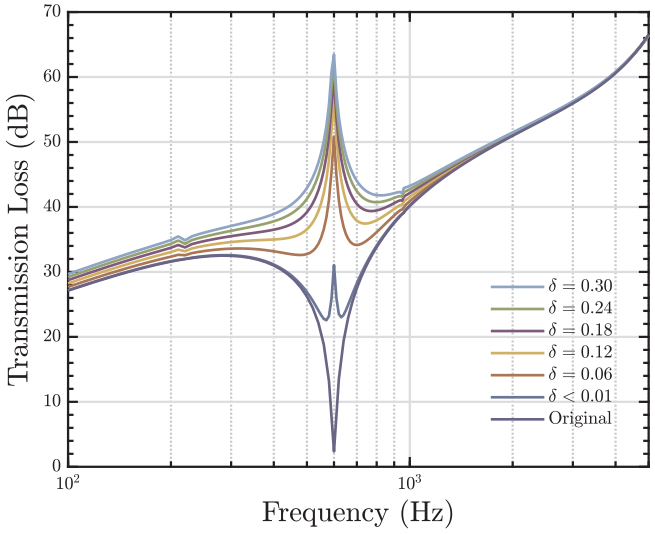

Fig. 8. Influence of the mass ratio on sound transmission loss and working frequency band.

theoretical estimate are different. Since the influence of the stepped resonators is only introduced by the effective mass theory, the radiated sound from the stepped resonators is not included in the theoretical model, which may account, at least in part, for the difference between the two peaks. The FE results indicate that the radiated sound from the resonators may potentially reduce the effectiveness of the current configuration at the resonance frequency.

3.3. Influences from the stepped resonators

The results so far have shown, both theoretically and numerically, that metamaterial sandwich plates including stepped resonators have the potential to compensate for the coincidence effect. However, the radiation from the stepped resonators mounted on the host sandwich plate might be an issue affecting the effectiveness, especially when the resonators are at resonance. This is however not captured by the theoretical model, and the FE simulations are therefore used in the following. In particular, ways to extend the bandwidth of the working frequency range are discussed.

A key parameter in order to extend the working frequency band is to increase the mass ratio of the stepped resonator to the host plate. Two options may be considered. First, to use heavier materials for the resonator; second to design larger resonators.

3.3.1. Influence of the mass ratio δ

A parametric study of resonators including small-volume, increasing masses, mounted on the outer surface of the sandwich, is conducted. The mass ratio is estimated as the ratio of the mass of the resonator to the mass of the host plate within each lattice.

As shown in Fig. 8, the working frequency band, as expected, is significantly broadened as the mass ratio increases. The STL within the working frequency band is also improved, at and around the resonance frequency. Below the coincidence frequency, where the mass law dominates, the STL is also improved with increasing masses since the overall surface density is increased by a factor $(1 + \delta)$. Above the coincidence frequency, however, the STLs with the different mass ratios converge to the same level as the host sandwich plate. The reason is here associated with the fact that the effective surface density is approaching that of the host plate, and that the STL above the coincidence frequency is also controlled by the stiffness of the plate.

Steering the mass ratio exclusively with the choice of material density is however unrealistic for practical applications (limited to choices such as steel, lead of tungsten in the literature). Larger resonators need therefore to be considered despite the potentially added sound radiation.

3.3.2. Effect of radiation

It may be expected that the sound radiation from larger resonators may adversely affect the STL properties of the metamaterial sandwich plate.

This point is considered by studying the influence of resonators with an increasing volume while keeping the mass ratio constant. The parameter σ represents the surface ratio of the resonator to the lattice. Only the sound intensity normal to the interface between the resonator and the surrounding medium contributes to the sound radiation.

In the analytical estimation, the radiation from the resonators is not included. In practice, when the resonators are mounted on the surface, the radiation from the resonators may have a substantial influence if the size of the resonator is relatively large compared to the size of the lattice, since the amplitude of the vibration velocity is large at resonance. As shown in Fig. 9, for a set mass ratio of 0.1, as the size of the resonator increases, the radiation effect will adversely affect the STL

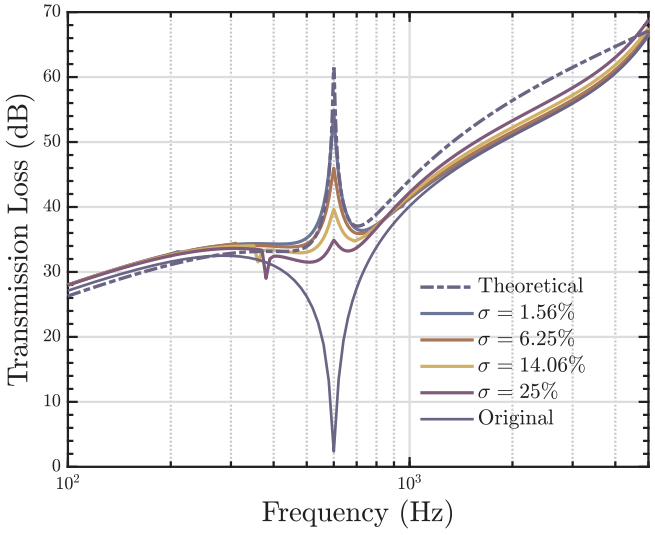

Fig. 9. Influence from the radiation of the stepped resonators on the sound transmission loss. σ represents the ratio of the surface area occupied by the stepped resonator to the surface of the host plate, with $\delta = 0.1$.

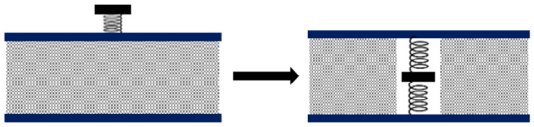

Fig. 10. Schematic of two designs of metamaterial sandwich plate: by having stepped resonators on the sandwich plate (Surface-mounted) and by embedding stepped resonators into the air inclusion of the sandwich plate (Embedded).

behavior at and close to the resonance frequency.

4. Embedded resonator

There are obvious limitations to increasing the mass ratio with either larger masses or denser material: *(i)* the higher the mass ratio, the heavier the plate (*e.g.* with $\delta = 0.3$, the surface density of the metamaterial sandwich plate may reach 73.84 kg/m^2.), and *(ii)* it may be impractical for most engineering applications to have a design with resonators mounted outside the sandwich (*e.g.* durability, practicality of a flat surface, etc.).

For these reasons, a design taking advantage of the sandwich configuration is proposed. In this sandwich configuration, the resonator is inserted inside the sandwich structure. The surface density is further kept constant at 56.8 kg/m^2 by compensating for the mass of the resonator with the removal of a corresponding mass of the core material, as shown in Fig. 10. Such a configuration is expected to maintain the static properties of the sandwich plate as the core material is not necessarily required to support the skin layers uniformly (e.g. honeycomb sandwich plate).

Several advantages may be expected from this configuration. First, it breaks from the limitation associated with a reduced set of materials to choose from in order to increase the mass ratio. Second, the radiation effect can be suppressed by encapsulating the resonator inside the structure. Third, the configuration with the flat surface is more realistic for practical applications while still benefiting from some properties of sandwich structures including low mass and high stiffness.

Fig. 11 shows the FE results of the STLs of the surface-mounted and the embedded metamaterial sandwich plates. The theoretical result is also plotted for comparison. The material of the resonator is chosen to be lead. The mass ratio is set to 0.1. As shown in Fig. 11, the STL performance is much better with the embedded configuration at resonance. The matching results between the theoretical estimation and the FE model at the resonance confirm that the radiation from the resonator is suppressed with the embedded configuration. Beyond the coincidence range, however, the STL performance of the second configuration decreases. This reduction of the performance may be attributed to the reduction of the effective mass. In fact, in this frequency range beyond the coincidence region, the effective mass of the metamaterial sandwich plate tends to the mass of the host sandwich plate. In the configuration proposed, where the resonator is inserted in a cavity within the core material of the sandwich, the overall mass of the host sandwich plate is reduced, which may explain this decrease in STL.

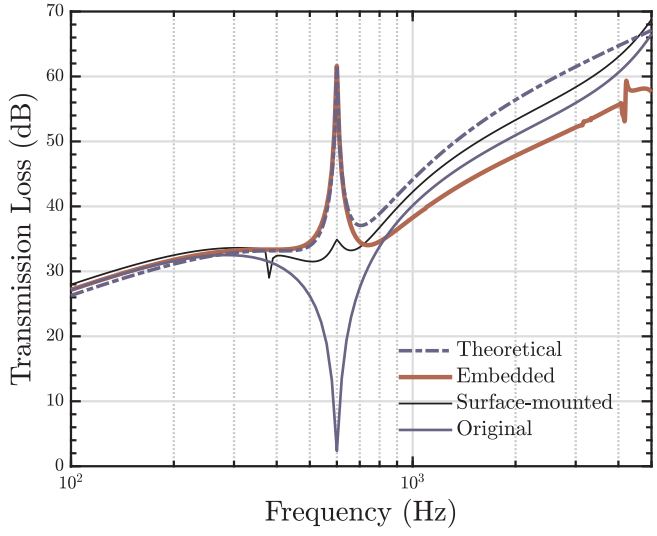

Fig. 11. Sound transmission loss of the surface-mounted metamaterial sandwich plate and the embedded metamaterial sandwich plate.

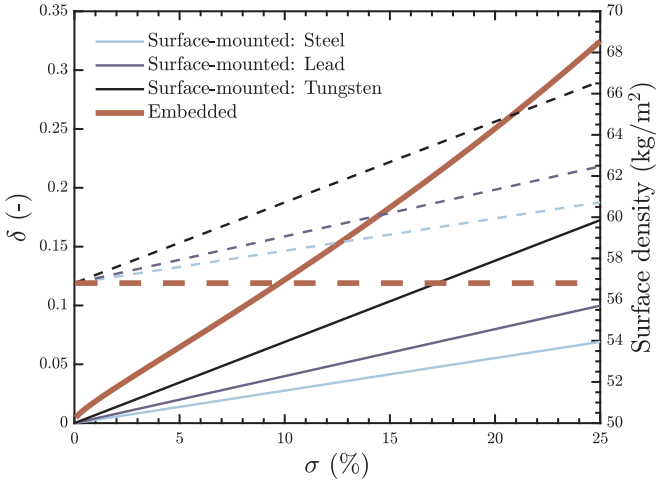

Fig. 12. Influence and limitation of the material that is used for fabricating the stepped resonator on the mass ratio and the surface density. σ is the surface ratio occupied by resonator. Solid lines correspond to the mass ratio δ; dashed lines represent the surface density.

Fig. 12 shows how the different materials influence the mass ratio and the surface density, both for the surface-mounted design and the embedded configurations. As can be seen from Fig. 12, for the surface-mounted design, when the surface ratio σ increases, both the mass ratio δ (solid line) and the surface density (dashed line) increase as well. However, the proposed embedded design allows to find a configuration where, as the surface ratio σ increases:

- the mass ratio increases faster than for any of the materials chosen for the surface-mounted configuration,
- it is possible to have a configuration where the surface density remains constant.

The bandwidth of the working frequency range of the embedded metamaterial sandwich plate is further evaluated with respect to the mass ratio δ. In the present case, the size of the air inclusion is set not to exceed half of the edge length of the lattice, i.e. a maximum value for δ of 0.325. As shown in Fig. 13, the working frequency band is extended as δ increases, at the expense of a reduction of the STL for frequencies beyond the coincidence.

However, the STL for higher frequencies remains higher than for low frequencies, which leads to an overall improved performance of the sandwich with higher mass ratio. Furthermore, in agreement with Eq. (17), this higher mass ratio implies a suitability for a broader range of frequencies for the coincidence phenomenon associated with different angles of incidence. This ensures the possibility of designing sandwich panels with both improved STL levels and working frequency band in the low frequency range, while keeping the overall mass constant, an essential point for high performance noise reduction solutions.

5. Conclusion

In the present contribution, a new design for metamaterial sandwich plates is studied, by encapsulating stepped resonators inside the

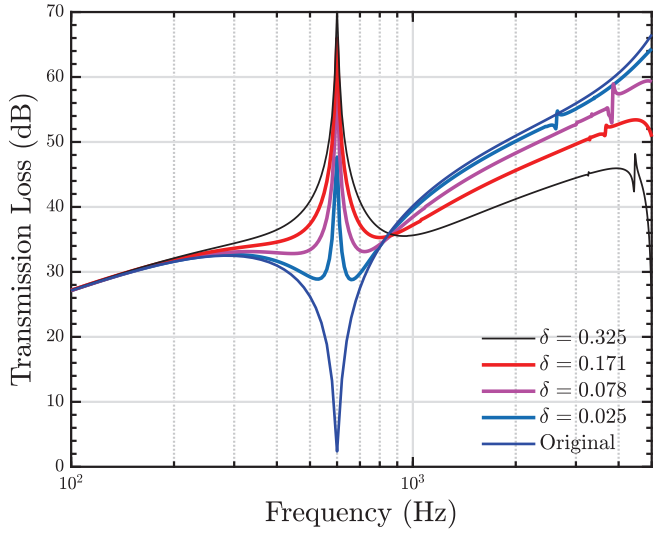

Fig. 13. Influence of the mass ratio on sound transmission loss in the embedded design.

sandwich panel. This configuration with internal resonators allows to improve the STL properties of the panel, in particular in the coincidence region. The study is conducted in combination with an analytical model based on an impedance approach. These theoretical developments support both the physical interpretation, and the fine tuning of the resonators in order to suppress the coincidence phenomenon. The associated STL estimates have proved to be in good agreement with the results from FE simulations below and at the coincidence frequency.

The influence of the resonator is then further studied with FE models, in which the radiation from the resonators is taken into account. In line with the literature [28], it is confirmed that the bandwidth of the working frequency band associated with the stepped resonators is strongly dependent on the mass ratio δ. Further, the results highlight that the radiation effect of the resonators may affect the STL property, especially at the resonance.

The proposed configuration is however shown to overcome the radiated sound from these resonators by embedding them in the core material. The resulting design further enables to preserve mechanical functionalities of the outer sheets as flat surfaces, thus making it a more realistic solution than most of the locally resonant metamaterial panels studied in the literature. It is also shown that the coincidence phenomenon is successfully overcome, allowing to extend the working frequency band while maintaining the static mechanical properties.

While the results are shown for oblique incidence configurations with a single targeted frequency range, the extension to diffuse field is straightforward, and multi-resonator solutions are currently under investigation.

Acknowledgments

The authors are grateful for the financial support provided by the KTH-CSC Programme (No. 201403170345). The Swedish Research Council (VR Grant 2015-04925) and the Centre for ECO2 Vehicle Design (Sweden's Innovation Agency VINNOVA, Grant Number 2016-05195) are gratefully acknowledged for their financial support of the second author.

References

[1] Kurtze G, Watters B. New wall design for high transmission loss or high damping. J Acoust Soc Am 1959;31(6):739–48.
[2] Ford R, Lord P, Walker A. Sound transmission through sandwich constructions. J Sound Vibr 1967;5(1):9–21.
[3] Dym CL, Ventres CS, Lang MA. Transmission of sound through sandwich panels: a reconsideration. J Acoust Soc Am 1976;59(2):364–7.
[4] Makris SE, Dym CL, Smith JM. Transmission loss optimization in acoustic sandwich panels. J Acoust Soc Am 1986;79(6):1833–43.
[5] Nilsson AC. Wave propagation in and sound transmission through sandwich plates. J Sound Vib 1990;138(1):73–94.
[6] Franco F, De Rosa S, Polito T. Finite element investigations on the vibroacoustic performance of plane plates with random stiffness. Mech Adv Mater Struct 2011;18(7):484–97.
[7] D'Alessandro V, Petrone G, Franco F, De Rosa S. A review of the vibroacoustics of sandwich panels: models and experiments. J Sandwich Struct Mater 2013;15(5):541–82.
[8] De Rosa S, Capobianco M, Nappo G, Pagnozzi G. Models and comparisons for the evaluation of the sound transmission loss of panels. Proc Inst Mech Eng, Part C: J Mech Eng Sci 2014;228(18):3343–55.
[9] Liu Z, Zhang X, Mao Y, Zhu Y, Yang Z, Chan CT, et al. Locally resonant sonic materials. Science 2000;289(5485):1734–6.
[10] Ma G, Sheng P. Acoustic metamaterials: from local resonances to broad horizons. Sci Adv 2016;2(2):e1501595.
[11] Cummer SA, Christensen J, Alù A. Controlling sound with acoustic metamaterials. Nat Rev Mater 2016;1:16001.
[12] Yang Z, Mei J, Yang M, Chan N, Sheng P. Membrane-type acoustic metamaterial with negative dynamic mass. Phys Rev Lett 2008;101(20):204301.
[13] Ho KM, Cheng CK, Yang Z, Zhang X, Sheng P. Broadband locally resonant sonic shields. Appl Phys Lett 2003;83(26):5566–8.
[14] Wang G, Wen X, Wen J, Shao L, Liu Y. Two-dimensional locally resonant phononic crystals with binary structures. Phys Rev Lett 2004;93(15):154302.
[15] Cummer SA, Schurig D. One path to acoustic cloaking. New J Phys 2007;9(3):45.
[16] Yang Z, Dai H, Chan N, Ma G, Sheng P. Acoustic metamaterial panels for sound attenuation in the 50–1000 Hz regime. Appl Phys Lett 2010;96(4):041906.
[17] Collet M, Ouisse M, Ichchou M, Ohayon R. Semi-active optimization of 2d wave's dispersion into shunted piezocomposite systems for controlling acoustic interaction. ASME 2011 Conference on Smart Materials, Adaptive Structures and Intelligent Systems, American Society of Mechanical Engineers 2011. p. 79–87.
[18] Hsu J-C. Local resonances-induced low-frequency band gaps in two-dimensional phononic crystal slabs with periodic stepped resonators. J Phys D: Appl Phys 2011;44(5):055401.
[19] Mei J, Ma G, Yang M, Yang Z, Wen W, Sheng P. Dark acoustic metamaterials as super absorbers for low-frequency sound. Nat Commun 2012. [ncomms1758].
[20] Bückmann T, Thiel M, Kadic M, Schittny R, Wegener M. An elasto-mechanical unfeelability cloak made of pentamode metamaterials. Nat Commun 2014;5:4130.
[21] Zhang H, Wen J, Xiao Y, Wang G, Wen X. Sound transmission loss of metamaterial thin plates with periodic subwavelength arrays of shunted piezoelectric patches. J Sound Vib 2015;343:104–20.
[22] Zhang H, Xiao Y, Wen J, Yu D, Wen X. Ultra-thin smart acoustic metasurface for low-frequency sound insulation. Appl Phys Lett 2016;108(14):141902.
[23] Fang X, Wen J, Bonello B, Yin J, Yu D. Ultra-low and ultra-broad-band nonlinear acoustic metamaterials. Nat Commun 2017;8(1):1288.
[24] Wang T, Sheng M, Qin Q. Sound transmission loss through metamaterial plate with lateral local resonators in the presence of external mean flow. J Acoust Soc Am 2017;141(2):1161–9.
[25] Climente A, Gao P, Wu L, Sánchez-Dehesa J. Scattering of flexural waves from an n-beam resonator in a thin plate. J Acoust Soc Am 2017;142(5):3205–15.
[26] Badreddine Assouar M, Senesi M, Oudich M, Ruzzene M, Hou Z. Broadband plate-type acoustic metamaterial for low-frequency sound attenuation. Appl Phys Lett 2012;101(17):173505.
[27] Xiao Y, Wen J, Wen X. Flexural wave band gaps in locally resonant thin plates with periodically attached spring–mass resonators. J Phys D: Appl Phys 2012;45(19):195401.
[28] Xiao Y, Wen J, Wen X. Sound transmission loss of metamaterial-based thin plates with multiple subwavelength arrays of attached resonators. J Sound Vib 2012;331(25):5408–23.
[29] Oudich M, Zhou X, Badreddine Assouar M. General analytical approach for sound transmission loss analysis through a thick metamaterial plate. J Appl Phys 2014;116(19):193509.
[30] Chen J, Sharma B, Sun C. Dynamic behaviour of sandwich structure containing spring-mass resonators. Compos Struct 2011;93(8):2120–5.
[31] Song Y, Feng L, Wen J, Yu D, Wen X. Reduction of the sound transmission of a periodic sandwich plate using the stop band concept. Compos Struct 2015;128:428–36.
[32] Heckl M. The tenth sir richard fairey memorial lecture: sound transmission in buildings. J Sound Vib 1981;77(2):165–89.
[33] Moore J, Lyon R. Sound transmission loss characteristics of sandwich panel constructions. J Acoust Soc Am 1991;89(2):777–91.
[34] Nilsson E, Nilsson A. Prediction and measurement of some dynamic properties of sandwich structures with honeycomb and foam cores. J Sound Vibr 2002;251(3):409–30.